Methylidyne Complexes Prepared by Reactions of Laser-Ablated Os Atoms with Methane, Methyl Halides, and Ethane: Observation of the C—H and Os—H Stretching Absorptions

Han-Gook Cho and Lester Andrews*

Department of Chemistry, University of Incheon, 177 Dohwa-dong, Nam-ku, Incheon, 402-749, South Korea, and Department of Chemistry, University of Virginia, P.O. Box 400319, Charlottesville, Virginia 22904-4319

Received October 17, 2007

Simple Os carbyne complexes ($HC{\equiv}OsH_3$, $HC{\equiv}OsH_2F$, $HC{\equiv}OsH_2Cl$, $HC{\equiv}OsH_2Br$, and $CH_3C{\equiv}OsH_3$) are produced in reactions of laser-ablated Os atoms with small alkanes and methyl halides via oxidative C—H insertion and α-hydrogen migration. The diagnostic methylidyne C—H stretching absorptions of $HC{\equiv}OsH_3$ and its halide derivatives are observed about 200 cm^{-1} above the precursor C—H stretching bands, and the frequencies are consistent with s character in hybridization in the C—H bond. The methylidyne complexes all have computed C_s structures, and particularly the $HC{\equiv}OsH_3$ and $CH_3C{\equiv}OsH_3$ complexes have two equivalent shorter and one longer Os—H bonds, parallel to the case of Re in similar complexes. The strong unique Os—H stretching absorption at an exceptionally low frequency is traced to the stretching mode of the long Os—H bond and antibonding character in the doubly occupied HOMO.

Introduction

The activation of C—H bonds has become a most important area in organometallic chemistry.[1] The discovery of transition-metal complexes with carbon−metal multiple bonds has catalyzed new developments in this area.[2] Subsequently numerous carbyne complexes have been reported;[2,3] however, only a few of them contain the simple M≡C—H or M≡C—CH_3 moiety (M = transition metal).[4] In addition, the weak methylidyne C—H stretching bands are normally covered by other much stronger absorptions in this frequency region. As a result, the methylidyne C—H vibrational characteristics remain largely uninvestigated despite various efforts while the stronger bands in the C≡M stretching region are frequently used as a probe to study ligand effects.[5,6]

In contrast to the large number of examples of alkylidyne complexes for the group 6 metals and a number for Re, there are relatively few osmium carbyne complexes.[2] Several of these and their reactions have been investigated by the Esteruelas group.[7]

Recently Hopkins et al. have measured methylidyne C—H stretching modes near 2980 cm^{-1} with deuterium counterpart at 2240 cm^{-1} structural dimensions of the H—C≡W moiey.[8] More recently small carbyne complexes ($HC{\equiv}ReH_3$, $HC{\equiv}ReH_2X$, $HC{\equiv}ReHX_2$ [X = F, Cl, and Br], and $CH_3C{\equiv}ReH_3$) have been prepared in reactions of laser-ablated Re atoms with methane, methyl and methylene halides, and ethane.[9] The methylidyne C—H stretching absorptions are observed and the trend of increasing frequency with the s character in the C—H bond is reported. The low symmetry structures of $HC{\equiv}ReH_3$, $CH_3C{\equiv}ReH_3$, and $HC{\equiv}ReX_3$ result from the Jahn–Teller effect[10] in the simple complexes.[11] Low symmetry structures are also observed for heavily halogenated derivatives such as $ClC{\equiv}ReCl_3$ and $FC{\equiv}ReCl_3$, which show exceptionally high C—X stretching frequencies.[11]

The C—H activation by laser-ablated transition-metal atoms has recently introduced many small carbene and carbyne complexes, which show interesting structures and fascinating photochemistry.[12] Here, we report the IR spectra of isotopic

* Author to whom correspondence should be addressed at the University of Virginia. E-mail: lsa@virginia.edu.

(1) (a) Campos, K. R. *Chem. Soc. Rev.* **2007**, *36*, 1069. (b) Díaz-Requejo, M. M.; Belderrain, T. R.; Nicasio, M. C.; Pérez, P. *Dalton Trans.* **2006**, 5559.

(2) (a) Schrock, R. R. *Chem. Rev.* **2002**, *102*, 145. (b) Herndon, J. W. *Coord. Chem. Rev.* **2007**, *251*, 1158. (c) Herndon, J. W. *Coord. Chem. Rev.* **2006**, *250*, 1889. (d) Herndon, J. W. *Coord. Chem. Rev.* **2005**, *249*, 999. (e) Herndon, J. W. *Coord. Chem. Rev.* **2004**, *248*, 3. (f) Da Re, R. E.; Hopkins, M. D. *Coord. Chem. Rev.* **2005**, *249*, 1396.

(3) (a) Fischer, E. O.; Kreis, G.; Kreiter, C. G.; Müller, J.; Huttner, G.; Lorenz, H. *Angew. Chem., Int. Ed. Engl.* **1973**, *12*, 564. (b) McLain, S. J.; Wood, C. D.; Messerle, L. W.; Schrock, R. R.; Hollander, F. J.; Youngs, W. J.; Churchill, M. R. *J. Am. Chem. Soc.* **1978**, *100*, 5962.

(4) Nugent, W. A.; Mayer, J. M. *Metal−Ligand Multiple Bonds*; John Wiley and Sons: New York, 1988.

(5) Barnes, D.; Gillett, D. A.; Merer, A. J.; Metha, G. F. *J. Chem. Phys.* **1996**, *105*, 6168. (W≡CH spectrum).

(6) (a) Barnes, M.; Merer, A. J.; Metha, G. F. *J. Mol. Spectrosc.* **1997**, *181*, 168. (Ti≡CH). (b) Sari, L.; Yamaguchi, Y.; Schaefer, H., III. *J. Chem. Phys.* **2001**, *115*, 5932. (HC≡Ge). (c) Kalemos, A.; Dunning, T. H., Jr.; Harrison, J. F.; Mavridis, A. *J. Chem. Phys.* **2003**, *119*, 3745. (Ti≡CH). (d) Fujitake, M.; Echizenya, R.; Shirai, T.; Kurita, S.; Ohashi, N. *J. Mol. Spectrosc.* **2004**, *223*, 113. (HC≡Si).

(7) (a) Baya, M.; Esteruelas, M. A. *Organometallics* **2002**, *21*, 2332. and references cited therein. (b) Barrio, P.; Esteruelas, M. A.; Onare, E. *Organometallics* **2002**, *21*, 2491. and references cited therein.

(8) (a) Manna, J.; Dallinger, R. F.; Miskowski, V. M.; Hopkins, M. D. *J. Phys. Chem. B* **2000**, *104*, 10928. (H—C≡W group freq). (b) Ménoret, C; Spasojević-de Bire, A.; Dao, N. Q.; Cousson, A.; Kiat, J.-M.; Manna, J. D.; Hopkins, M. D. *J. Chem. Soc., Dalton Trans.* **2002**, 3731. (BrW≡CH-(dmpe-d_{12})$_2$).

(9) (a) Cho, H.-G.; Andrews, L. *Organometallics* **2007**, *26*, 4098. (b) Cho, H.-G.; Andrews, L. *Inorg. Chem.* , . published online Feb. 8, http://dx.doi.org/10.1021/ic701505w, and references cited therein.

(10) (a) Jahn, H. A.; Teller, E. *Proc. R. Soc. London, A* **1937**, *161*, 220. (b) Teller, E. A historical note. In *The Jahn-Teller Effect in Molecules and Crystals*; Engelman, R., Ed.; Wiley-Interscience: London, 1972.

(11) Lyon, J. T.; Cho, H.-G.; Andrews, L.; Hu, H.-S.; Li, J. *Inorg. Chem.* **2007**, *46*, 8728.

(12) Andrews, L.; Cho, H.-G. *Organometallics* **2006**, *25*, 4040. and references therein (Review article).

10.1021/om701041u CCC: $40.75
Publication on Web 03/05/2008

products from reactions of laser-ablated Os atoms with methane, methyl halides, and ethane. The major methylidyne products reveal the elusive methylidyne C—H stretching absorptions, and computations predict the low symmetry structures. These simple osmium hydride methylidyne complexes are fundamentally important as they can be investigated by high-level theoretical methods to understand the unique bonding and structure around Os,[7,13] which is one of the most important metals in organometallic chemistry.

Experimental and Computational Methods

Laser-ablated Os atoms (Metallium) were reacted with CH_4 (Matheson, UHP grade), $^{13}CH_4$, CD_4, CH_2D_2 (Cambridge Isotopic Laboratories), (CH_3F, CH_3Cl, CH_3Br, (Matheson), CD_3F (synthesized from CD_3Br and HgF_2)), $^{13}CH_3F$, CD_3Br (Cambridge Isotopic Laboratories, 99%), and CD_3Cl (synthesized from CD_3Br and $HgCl_2$) in excess argon during condensation at 8 K, using a closed-cycle refrigerator (Air Products HC-2). These methods have been described in detail elsewhere.[14] Reagent gas mixtures of 0.5–2.0% in argon were employed. After reaction, infrared spectra were recorded at a resolution of 0.5 cm^{-1}, using a Nicolet 550 spectrometer with an MCT-B detector. Samples were later irradiated for 20 min periods by a mercury arc street lamp (175 W) with the globe removed and a combination of optical filters, and subsequently annealed to allow further reagent diffusion.

Complementary density functional theory (DFT) calculations were carried out with the Gaussian 03 package,[15] B3LYP density functional,[16] 6-311++G(3df,3pd) basis sets for C, H, F, Cl, and Br,[17] and SDD pseudopotential and basis set[18] for Os to provide a consistent set of vibrational frequencies for the reaction products. Geometries were fully relaxed during optimization, and the optimized geometry was confirmed by vibrational analysis. Anharmonic frequency calculations by numerical differentiation[19] (with Gaussian 03 keyword "anharmonic") were also carried out with B3LYP to compare with experimental values and to examine the effects of anharmonicity. BPW91,[20] MP2,[21] and more rigorous CCSD[22] calculations were also done for selected molecules to confirm the B3LYP results. The vibrational frequencies were calculated analytically except for the CCSD calculations. Zero-point energy is included in the calculation of the binding energy of a metal complex.

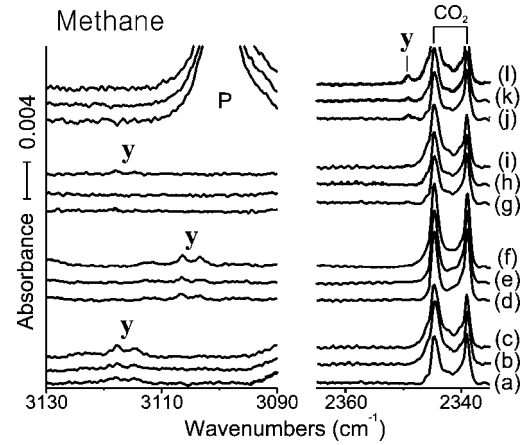

Figure 1. IR spectra in the C—H and C—D stretching regions for the laser-ablated Os atom reaction product with CH_4 in excess argon at 8 K: (a) Os + 1.0% CH_4 in Ar codeposited for 1 h; (b) after photolysis ($\lambda > 420$ nm); (c) after photolysis ($240 < \lambda < 380$ nm); (d) Os + 1.0% $^{13}CH_4$ in Ar; (e) after photolysis ($\lambda > 420$ nm); (f) after photolysis ($240 < \lambda < 380$ nm). (g) Os + 2.0% CH_2D_2 in Ar; (h) after photolysis ($\lambda > 220$ nm); (i) after photolysis ($240 < \lambda < 380$ nm); (j) Os + 1.0% CD_4 in Ar; (k) after photolysis ($\lambda > 220$ nm); (l) after photolysis ($240 < \lambda < 380$ nm). **y** denotes the methylidyne product absorption. P and CO_2 stand for methane precursor and residual CO_2 absorptions, respectively.

Results and Discussion

Infrared spectra and supporting quantum chemical structure and frequency calculations will be presented for the major products of Os atom reactions with methane, methyl halides, and ethane in turn. Often bands are observed that are common to a particular hydrocarbon precursor, using different metal atoms, and many of these have been identified in previous studies.[9,12]

Os + CH_4. Recent work on the reaction of Re atoms and methane produced diagnostic absorptions at 3101.8 and 1809.9 cm^{-1}, which were assigned to the rhenium trihydride methylidyne complex.[9] The C—H and C—D stretching regions in the infrared spectra for the products of laser-ablated Os atoms with CH_4, $^{13}CH_4$, CD_4, and CH_2D_2 are shown in Figure 1. Only one group of product absorptions is observed on the basis of their behaviors on photolysis and annealing. The product absorptions at 3117.8 and 3114.7 cm^{-1}, marked "**y**" for methylidyne, decrease slightly on vis ($\lambda > 420$ nm) and double on UV ($240 < \lambda < 380$ nm) photolysis. The C—H stretching absorptions are split by interaction with the matrix cage, and the ^{13}C counterparts are found equally split at 3106.3 and 3103.3 cm^{-1} ($^{12}C/^{13}C$ ratios of both 1.004), respectively. One deuterium counterpart is observed at 2349.1 cm^{-1} just above CO_2 impurity in the matrix (H/D ratio of 1.327). The observed frequencies are summarized in Table 1. The C—H stretching absorption (3117.8 cm^{-1}) is 16 cm^{-1} higher in frequency than that for the analogous Re species.[9] Parallel to the Re case, the high C—H stretching frequency, which is about 200 cm^{-1} higher than those

(13) (a) Esteruelas, M. A.; Lahoz, F. J.; Lopez, J. A.; Oro, L. A.; Schlünken, C.; Valero, C.; Werner, H. *Organometallics* **1992**, *11*, 2035. (b) Aime, S.; Diana, E.; Gobetto, R.; Milanesio, M.; Valls, E.; Viterbo, D. *Organometallics* **2002**, *21*, 50.

(14) (a) Andrews, L.; Citra, A. *Chem. Rev.* **2002**, *102*, 885. and references therein. (b) Andrews, L. *Chem. Soc. Rev.* **2004**, *33*, 123. and references therein.

(15) Kudin, K. N.; Burant, J. C.; Millam, J. M.; Iyengar, S. S.; Tomasi, J.; Barone, V.; Mennucci, B.; Cossi, M.; Scalmani, G.; Rega, N.; Petersson, G. A.; Nakatsuji, H.; Hada, M.; Ehara, M.; Toyota, K.; Fukuda, R.; Hasegawa, J.; Ishida, M.; Nakajima, T.; Honda, Y.; Kitao, O.; Nakai, H.; Klene, M.; Li, X.; Knox, J. E.; Hratchian, H. P.; Cross, J. B.; Adamo, C.; Jaramillo, J.; Gomperts, R.; Stratmann, R. E.; Yazyev, O.; Austin, A. J.; Cammi, R.; Pomelli, C.; Ochterski, J. W.; Ayala, P. Y.; Morokuma, K.; Voth, G. A.; Salvador, P.; Dannenberg, J. J.; Zakrzewski, V. G.; Dapprich, S.; Daniels, A. D.; Strain, M. C.; Farkas, O.; Malick, D. K.; Rabuck, A. D.; Raghavachari, K.; Foresman, J. B.; Ortiz, J. V.; Cui, Q.; Baboul, A. G.; Clifford, S.; Cioslowski, J.; Stefanov, B. B.; Liu, G.; Liashenko, A.; Piskorz, P.; Komaromi, I.; Martin, R. L.; Fox, D. J.; Keith, T.; Al-Laham, M. A.; Peng, C. Y.; Nanayakkara, A.; Challacombe, M.; Gill, P. M. W.; Johnson, B.; Chen, W.; Wong, M. W.; Gonzalez, C.; Pople, J. A. *Gaussian 03*, Revision B.04, Gaussian, Inc.: Pittsburgh, PA, 2003.

(16) (a) Becke, A. D. *J. Chem. Phys.* **1993**, *98*, 5648. (b) Lee, C.; Yang, Y.; Parr, R. G. *Phys. Rev. B* **1988**, *37*, 785.

(17) Raghavachari, K.; Trucks, G. W. *J. Chem. Phys.* **1989**, *91*, 1062.

(18) Andrae, D.; Haeussermann, U.; Dolg, M.; Stoll, H.; Preuss, H. *Theor. Chim. Acta* **1990**, *77*, 123.

(19) Page, M.; Doubleday, C.; McIver, J. W, Jr. *J. Chem. Phys.* **1990**, *93*, 5634.

(20) Burke, K.; Perdew, J. P.; Wang, Y. In *Electronic Density Functional Theory: Recent Progress and New Directions*; Dobson, J. F., Vignale, G., Das, M. P., Eds.; Plenum: New York, 1998.

(21) Frisch, M. J.; Head-Gordon, M.; Pople, J. A. *Chem. Phys. Lett.* **1990**, *166*, 281.

(22) Pople, J. A.; Krishnan, R.; Schlegel, H. B.; Binkley, J. S. *Int. J. Quantum Chem.* **1978**, *14*, 545.

Table 1. Frequencies of Product Absorptions Observed from the Reaction of Methane with Os in Excess Argon[a]

CH_4	CD_4	$^{13}CH_4$	CH_2D_2	description
3117.8, 3114.7	2349.1	**3106.3**, 3103.3	**3118.0**, 3114.4, 2349.1	C−H str.
2235.6	1607.7	2235.6		OsH_2 str.
2003.2, 1999.0, **1996.0**		1996.0		OsH_2 str.
1860.5, 1852.3, **1848.7**, 1845.2, 1837.5, 1824.7	1332.4, **1330.2**, 1328.3	1852.1, **1848.7**, 1845.1	**1847.4**, 1844.0, 1331.6	OsH str.
695.2				HCOs bend
644.8		covered		HCOs bend

[a] All frequencies are in cm^{-1}. Stronger absorptions in bold: additional bands are due to matrix site splittings of the major absorption. Description gives major vibrational coordinate.

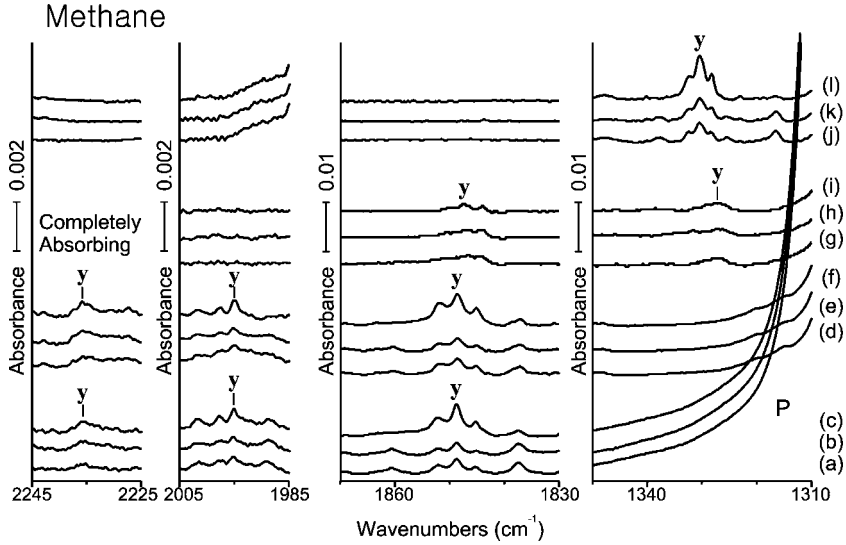

Figure 2. The Os−H and Os−D stretching regions in the IR spectra for the product of laser-ablated Os atom reaction with methane isotopomers in excess argon at 8 K and their variation on vis ($\lambda > 420$ nm) and UV ($240 < \lambda < 380$ nm) photolysis as described in the caption to Figure 1. P denotes methane precursor.

of normal saturated hydrocarbons, strongly indicates a multiple carbon−osmium bond providing higher s character to the C−H bond.[4,23] The same C−H and C−D stretching absorptions were observed within experimental error in the CH_2D_2 spectra, which indicates that no other C−H bond is in the proximity to perturb significantly the C−H stretching mode.

Shown in Figure 2 are the isotopic methane product spectra in the Os−H and Os−D stretching regions. The strongest product absorption by a factor of 5 is observed as a group of bands quite low in the 1800 cm^{-1} region. These absorptions are represented by the strong 1848.7 cm^{-1} band, which tracks with the above C−H stretching modes on irradiation and annealing, and the deuterium counterparts are similarly split by the matrix and represented by the dominant peak observed at 1330.2 cm^{-1} (H/D ratio 1.390). It is noteworthy that the similarly split ^{13}C counterparts show essentially no isotopic shifts. While these strong Os−H stretching absorptions indicate that oxidative C−H insertion by Os atom clearly occurs, the frequencies are much lower than the previously observed Os−H stretching frequencies (1994.5 and 1935.2 cm^{-1} for OsH_2[24] and normally 2100–2170 cm^{-1} for larger Os organometallic complexes with Os−H bonds[25]). Two other Os−H stretching absorptions, which are much weaker, are observed at 2235.6 and 1996.0 cm^{-1}, and the ^{13}C counterparts have the same frequencies. However, unfortunately the deuterium counterparts are not observed: the stronger, higher frequency one is believed overlapped by water residue absorptions and the lower one is simply too weak to be observed here.

The new Os−H stretching absorptions, along with the high-frequency C−H stretching bands, suggest a major product with a C−H group adjacent to a multiple carbon−osmium bond and other Os−H bonds, analogous to the $HC{\equiv}ReH_3$ species recently reported.[9] Our previous works with methane activation by transition-metal atoms show that there are three possible reaction products, monohydrido insertion, dihydrido, and trihydrido complexes.[12] The observed C−H and Os−H stretching bands suggest a trihydrido osmium complex, $HC{\equiv}OsH_3$, and the observed frequencies correlate with the predicted values for $HC{\equiv}OsH_3$ in its singlet ground state (Table 2). The C−H stretching frequency is calculated higher in the harmonic approximation by the wave function based CCSD and MP2 methods than by the density functional B3LYP, as expected.[26] Particularly the exceptionally high intensity and low frequcncy of the Os−H stretching band at 1848.7 cm^{-1} is well covered by three computations (e.g., CCSD frequency of 1870.7 cm^{-1} and intensity of 246 km/mol). Unfortunately these calculations do not account for anharmonicity, and the CCSD frequency for the lighter hydrogen isotope is 22 cm^{-1} higher than observed while the heavier deuterium isotopic calculated frequency is 1 cm^{-1} lower than observed owing to the neglect of anharmonicity. The generally good correlation between the observed and predicted vibrational characteristics substantiates formation of the simplest osmium methylidyne complex, $HC{\equiv}OsH_3$.

(23) Pavia, D. L.; Lampman, G. M.; George, S. K. *Introduction to Spectroscopy*, 3rd ed.; Brooks Cole: New York, 2000.

(24) Wang, X.; Andrews, L. Unpublished data.

(25) Bolano, T.; Castarienas, R.; Esteruelas, M. A.; Onare, E. *J. Am. Chem. Soc.* **2006**, *128*, 3965. (Os−H freq, Os−F complexes).

(26) (a) Scott, A. P.; Radom, L. *J. Phys. Chem.* **1996**, *100*, 16502. (b) Andersson, M. P.; Uvdal, P. L. *J. Phys. Chem. A* **2005**, *109*, 3937.

Table 2. Observed and Calculated Fundamental Frequencies of HC≡OsH_3 Isotopomers[a]

	HC≡OsH_3					DC≡OsD_3					H^{13}C≡OsH_3				
approx description	obsd	CCSD	int	MP2	B3LYP	obsd	CCSD	int	MP2	B3LYP	obsd	CCSD	int	MP2	B3LYP
A′ C—H str.	3117.8	3346.6	45	3326.0	3243.8	2349.1	2496.4	29	2477.9	2413.9	3106	3333.7	44	3313.4	3231.8
A′ OsH_2 str.	2235.6	2328.9	47	2341.6	2328.3	1607.7	1653.1	24	1661.7	1651.6	2235.6	2328.9	47	2341.6	2328.3
A′ OsH str.	1848.7	1870.7	246	1919.9	1902.7	1330.2	1328.9	120	1363.5	1352.2	1848.7	1870.7	247	1919.9	1902.6
A′ C≡ Os str.		1173.6	6	1134.8	1111.4		1109.8	4	1076.2	1051.0		1136.9	5	1099.1	1077.4
A′ OsH_3 deform		923.0	5	946.5	928.0		679.7	7	695.3	723.7		920.8	5	943.3	920.6
A′ OsH_2 bend		886.9	43	925.9	863.0		638.1	18	657.6	631.9		884.8	43	925.8	859.6
A′ HCOs bend	644.8	656.5	61	675.3	682.0		475.9	34	495.4	488.7	covered	655.2	60	673.3	681.2
A′ OsH_3 rock		412.2	49	427.9	653.3		310.9	26	324.5	465.0		409.6	48	425.0	653.3
A″ OsH_2 str.	1996.0	2278.5	11	2290.1	2097.6		1616.1	6	1623.9	1487.6	1996.0	2278.5	11	2290.2	2097.5
A″ OsH_2 twist		907.3	0	929.5	513.8		693.2	3	701.9	364.8		902.0	0	925.3	513.7
A″ HCOs bend	695.2	735.2	87	747.9	358.0		531.8	44	548.0	254.0		733.3	87	744.9	358.0
A″ OsH_3 rock		292.6	36	499.8	260.8		209.2	18	256.7	203.4		292.5	37	499.8	258.6

[a] Frequencies and intensities are in cm^{-1} and km/mol. Observed in an argon matrix. Harmonic frequencies and intensities are computed with 6-311++G(3df, 3pd), and the SDD core potential and basis set are used for Os. Intensities calculated with CCSD. HC≡OsH_3 has a C_s structure with two equal Os—H bonds with CCSD and MP2, but a C_1 structure with B3LYP. The symmetry notations are based on the C_s structure.

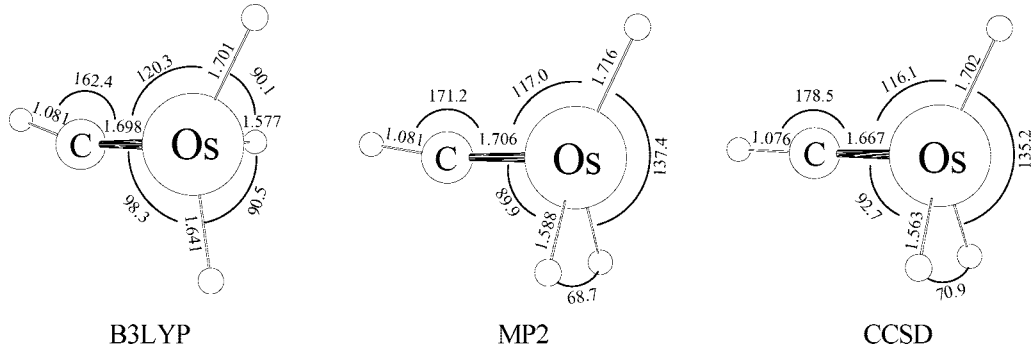

Figure 3. Predicted structure of HC≡OsH_3. Geometry optimization with B3LYP/6-311++G(3df,3pd) give a C_1 structure with highly distorted OsH_3 group, whereas MP2 and CCSD calculations lead to a C_s structure, where one of the Os—H bonds is significantly longer than the other two. The CCSD structure with C_s symmetry is similar to that of HC≡ReH_3 (ref 9).

On the other hand, the predicted vibrational characteristics for the insertion and dihydrido methylidene products do not agree with the observed values. For example, the insertion product in the triplet ground state would show three C—H stretching bands in the frequency range of 2960–2790 cm^{-1} and an Os—H stretching band at around 2100 cm^{-1} (the scale factor of 0.96 applied here only, see calculated frequencies in Table S1, Supporting Information). Figure S1 (Supporting Information) compares the spectra for Os reactions with methane and ethane in the 2300–1800 cm^{-1} region, which includes any possible Os—H stretching chromophore, and there are no significant bands that can be assigned to the insertion product. Furthermore, the dihydrido product in the singlet ground state would show two C—H stretching bands in the frequency range of 2940–2850 cm^{-1} and two Os—H stretching bands at around 2200 cm^{-1}. In addition, none of the absorptions would be unusually strong. Table S2 (Supporting Information) lists the CH_2=OsH_2 frequencies at the CCSD and B3LYP levels of theory, and substantiates our assertion that the methylidene complex is not responsible for the present major new product absorptions.

The C≡Os stretching mode, calculated in the 1100 cm^{-1} region (Table 2), is unfortunately too weak to observe here. Two additional weak absorptions are observed in the low-frequency region (Figure S2, Supporting Information), which exhibit the same behavior on irradiation and annealing as the above diagnostic C—H and Os—H stretching frequencies. These absorption at 695.2 and 644.8 cm^{-1} in the CH_4 spectrum are tentatively assigned to the A″ and A′ H—C—Os bending modes of HC≡OsH_3 as listed in Tables 1 and 2.

The structure of HC≡OsH_3 is shown in Figure 3 as computed with three different methods. While giving reasonable vibarational characteristics for the C—H and Os—H stretching bands, the B3LYP structure has C_1 symmetry and particularly the OsH_3 group is distorted (all three Os—H bonds are located on one side of the metal center). On the other hand, the MP2 and CCSD structures, in contrast to the B3LYP structure at the metal center, have C_s symmetry and are similar to each other. These structures clearly show that the two Os—H bonds are predicted to be equal and short, while the third Os—H bond is relatively much longer (e.g., 1.563 vs 1.702 Å in the CCSD structure). The C—Os—H angles are substantially different as well (e.g., 92.7° vs 116.1° in the CCSD structure). The exceptionally low Os—H stretching frequency arises from the long Os—H bond, and the high absorption intensity originates from the large negative charge on the unique hydrogen atom. (The CCSD calculation for Mulliken charge provides a good measure of the relative charges on the atoms in the molecule. This charge on the unique H is −0.45, which is compared with −0.17 for the two equivalent hydrogen atoms and is balanced by +1.39 on the Os center.)

The monohydrido insertion (CH_3—OsH) and the methylidene complex (CH_2=OsH_2) products in their triplet and singlet ground states are predicted to be 29 and 36 kcal/mol more stable than the reactants (Os(^{5}D) and CH_4) at the level of B3LYP/6-311++G(3df,3pd)/SDD. On the other hand, the trihydrido methylidyne product (HC≡OsH_3) in the singlet ground state is computed to be 34 kcal/mol lower in energy than the reactants at the B3LYP level of theory. However, the more rigorous CCSD calculation shows that the methylidyne is 7 kcal/mol lower in energy than the methylidene complex. Our previous

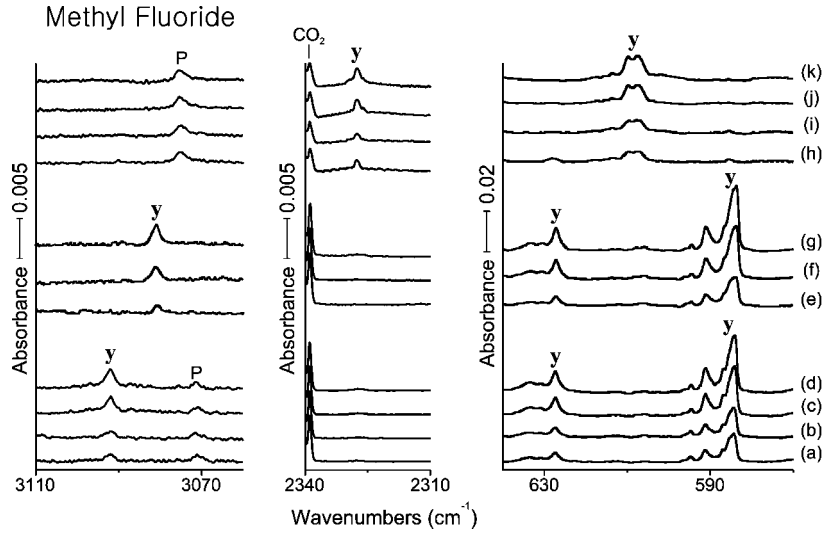

Figure 4. The C—H, C—D, and Os—F stretching regions for the laser-ablated Os atom reaction product with CH_3F in excess argon at 8 K and their variation on vis ($\lambda > 420$ nm), UV ($240 < \lambda < 380$ nm), and full arc ($\lambda > 220$ nm) photolysis: (a) Os + 0.5% CH_3F in Ar codeposited for 1 h; (b) after vis photolysis; (c) after UV photolysis; (d) after full arc photolysis; (e) Os + 0.5% $^{13}CH_3F$ in Ar codeposited for 1 h; (f) after UV photolysis; (g) after full arc photolysis; (h) Os + 0.5% CD_3F in Ar codeposited for 1 h; (i) after vis photolysis; (j) after UV photolysis; (k) after full arc photolysis. **y**, P, and CO_2 stand for the methylidyne product, precursor, and residual CO_2 absorptions, respectively.

Table 3. Observed and Calculated Fundamental Frequencies of HC≡OsH_2F Isotopomers[a]

	HC≡OsH_2F					DC≡OsD_2F					H^{13}C≡OsH_2F				
approx description	obsd	B3LYP, anh[b]	B3LYP	CCSD	int	obsd	B3LYP, anh[b]	B3LYP	CCSD	int	obsd	B3LYP, anh[b]	B3LYP	CCSD	int
A′C—H str.	3091.9	3101.8	3246.8	3325.3	23	2327.6	2339.7	2418.2	2479.0	17	3080.9	3090.5	3234.6	3312.7	23
A′ OsH_2 str.	*c*	2229.4	2321.0	2424.2	21		1600.9	1647.4	1721.0	11		2229.3	2321.0	2424.2	21
A′ C≡Os str.		1088.0	1102.0	1147.4	4		1035.3	1049.2	1090.7	3		1052.3	1065.4	1109.7	3
A′ HCOs bend	908.3	913.1	950.4	995.8	11		721.2	742.7	774.4	6		906.0	942.8	988.1	11
A′ OsH_2 scis.		773.2	747.6	787.5	20		540.1	530.3	557.7	5		773.3	747.6	787.4	20
A′ OsH_2 wag	627.4	617.0	640.8	687.5	55	449.2	433.5	447.3	481.6	73	627.1	616.9	640.2	686.6	55
A′ OsF str.	584.3	576.8	582.6	606.0	176	609.9	597.4	600.9	625.3	117	584.0	576.5	582.3	605.9	177
A′ COsF bend		139.5	142.6	152.7	6		132.1	133.7	143.5	5		137.6	140.4	150.3	6
A″ OsH_2 str.		2207.9	2295.4	2380.8	9		1583.7	1627.9	1688.4	5		2207.9	2295.4	2380.8	9
A″ HCOs bend		902.2	929.8	958.1	1		717.7	735.9	754.7	1		894.5	921.2	949.6	1
A″ OsH_2 twist	633.6	636.8	662.4	697.7	51		458.1	471.8	497.2	25	633.6	636.7	661.9	697.2	51
A″ OsH_2 rock		217.0	199.3	259.7	2		160.8	159.8	202.4	1		218.1	198.5	259.1	3

[a] Frequencies and intensities are in cm^{-1} and km/mol. Observed in an argon matrix. Harmonic frequencies are computed with B3LYP or CCSD/6-311++G(3df, 3pd), and the SDD core potential and basis set used for Os. Intensities are for CCSD. HC≡OsH_2F has a C_s structure with two equal Os—H bonds. The symmetry notations are based on the C_s structure. [b] Calculated anharmonic frequencies. [c] Covered by precursor band.

studies demonstrate that oxidative C—H insertion by the metal atom occurs first and hydrogen migration follows to form higher oxidation-state products.[12] Virtually exclusive formation of the methylidyne product suggests that the trihydrido complex (HC≡OsH_3) is in fact more stable in the matrix than the insertion (CH_3—OsH) and dihydrido (CH_2═OsH_2) products. Parallel to the case of Re, no other product is identified in the Os + CH_4 spectra, showing the strong tendency of osmium to form a carbon−osmium triple bond in reaction with methane. The variation in the structure depending on the computation method and the exceptional preference to form the methylidyne product in the reaction of Os with methane obviously require further investigation with higher levels of theoretical computations. Finally, the observation of split bands for the Os—H stretching fundamentals is probably in part due to ease of distortion of the structure around the metal center. In particular the extra absorptions around the strong 1848.7 cm^{-1} absorption are likely due to less stable HC≡OsH_3 structures, which are relaxed on sample irradiation.

Os + CH_3X. Shown in Figure 4 are the isotopic methyl fluoride spectra in the C—H and C—D stretching and low-frequency regions. The product absorption marked "**y**" doubles and increases another 100% on vis and UV photolysis (~300% in total), respectively. Methyl fluoride is more reactive with Os than methane, which results in the stronger common C—H stretching bands. The C—H stretching absorption is observed at 3091.9 cm^{-1}, which is 25.9 cm^{-1} lower than that in the CH_4 spectrum, and the D and ^{13}C counterparts are observed at 2327.6 and 3080.9 cm^{-1} (H/D and $^{12}C/^{13}C$ ratios of 1.328 and 1.004), respectively. The single isotopic C—H stretching absorptions again indicate formation of a product with a C—H moiety, and the frequency is again about 200 cm^{-1} higher than the C—H stretching frequency of the precursor and suggests a multiple carbon−osmium bond, which allocates a higher s-character to the C—H bond.

The product absorptions are attributed to HC≡OsH_2F, and the observed frequencies are compared with those predicted for the methylidyne complex in Table 3. The Os—H stretching absorptions of the halogenated methylidyne product are too weak to observe here. The absorption at 633.6 cm^{-1} shows negligible ^{13}C shift and is attributed to the OsH_2 twisting mode without observation of the D counterpart. The one at 627.4 cm^{-1} exhibits D and ^{13}C shifts of −178.2 cm^{-1} (not shown) (H/D ratios of 1.397) and −0.3 cm^{-1}, and it is assigned to the OsH_2 wagging

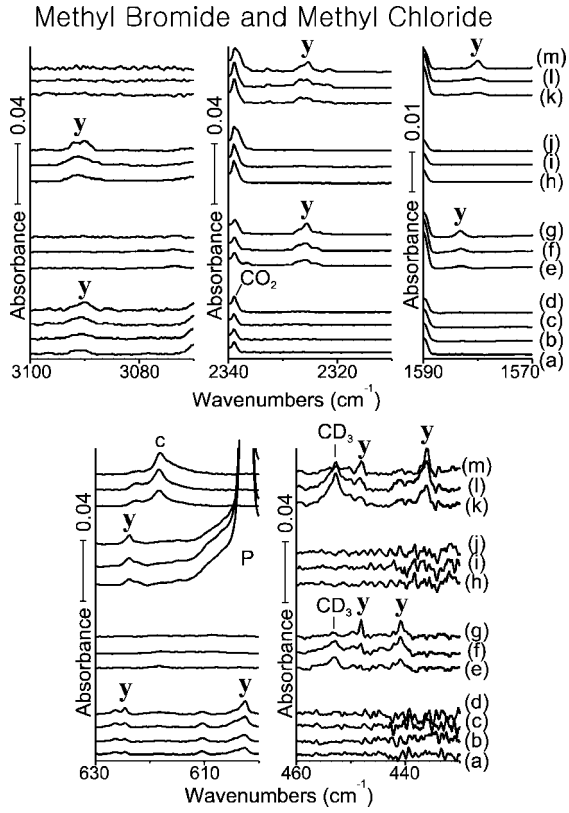

Figure 5. The C—H, C—D, and Os—D stretching and low-frequency regions for the laser-ablated Os atom reaction product with CH_3Cl and CH_3Br in excess argon at 8 K and their variation on photolysis and annealing: (a) Os + 0.5% CH_3Cl in Ar codeposited for 1 h; (b) after vis ($\lambda > 420$ nm) photolysis; (c) after UV ($240 < \lambda < 380$ nm) photolysis; (d) after annealing to 28 K; (e) Os + 0.5% CD_3Cl in Ar codeposited for 1 h; (f) after UV photolysis; (g) after annealing to 28 K; (h) Os + 0.5% CH_3Br in Ar codeposited for 1 h; (i) after UV photolysis; (j) after annealing to 28 K; (k) Os + 0.5% CD_3Br in Ar codeposited for 1 h; (l) after UV photolysis; (m) after annealing to 28 K. **y** and CO_2 stand for the methylidyne product and residual CO_2 absorptions, respectively. C and P designate common and precursor absorptions, respectively.

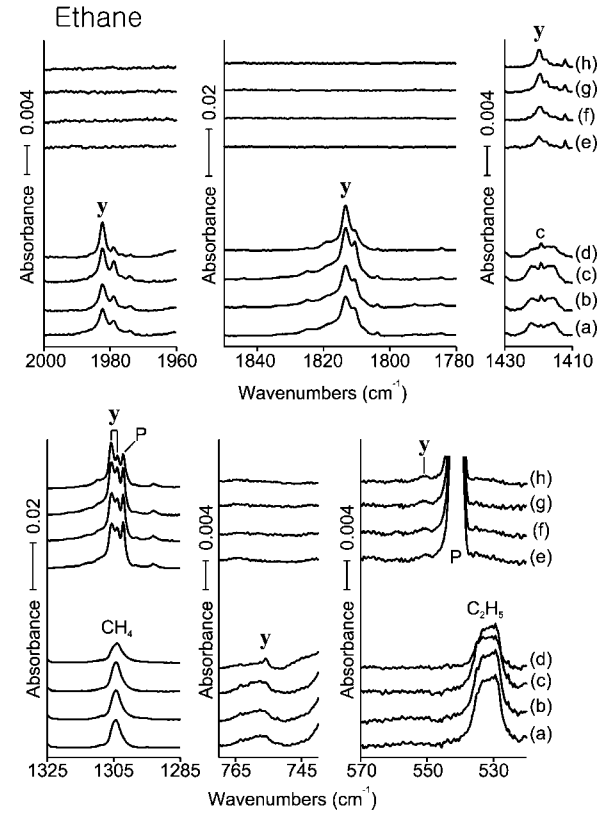

Figure 6. The Os—H and Os—D stretching and low-frequency regions for the laser-ablated Os atom reaction product with ethane in excess argon at 8 K and their variation on vis ($\lambda > 420$ nm) and UV ($240 < \lambda < 380$ nm) photolysis and annealing: (a) Os + 1.0% C_2H_6 in Ar codeposited for 1 h; (b) after vis photolysis; (c) after UV photolysis; (d) after annealing to 28 K; (e) Os + 1.0% C_2D_6 in Ar codeposited for 1 h; (f) after vis photolysis; (g) after UV photolysis; (h) after annealing to 28 K. **y**, P, and c stand for the methylidyne product, precursor, and common (in M + C_2H_6 spectra) absorptions, respectively.

mode. The strong absorption at 584.3 cm^{-1} has its site-split D counterpart at 609.9 and 607.4 cm^{-1} and ^{13}C counterpart at 584.0 cm^{-1}. Interaction between the OsH_2 wagging and Os—F stretching modes depresses the latter, but on deuteration this interaction is removed and the Os—F mode frequency increases. The 24 cm^{-1} increase in the Os—F stretching frequency on D substitution is compared with the 21 cm^{-1} increase in calculated anharmonic B3LYP frequencies in Table 3.

To date only a few Os—F organometallic compounds have been reported.[25] Moreover, osmium fluoro—carbyne complexes are uncommon.[27] Formation of this simple Os—F complex shows that reaction of laser-ablated Os atoms with a fluoroalkane is an effective way to produce Os fluoro-carbyne complexes. The C_s structure of HC≡OsH_2F is shown in Figure 7. The C—H insertion products and higher oxidation complexes form via following H migration studied previously normally show strong metal—hydrogen stretching bands. The unusually low absorption intensities of the Os—H stretching bands are traced to the low atomic charges on the hydrogen atoms bonded to the Os atom (B3LYP Mulliken charge of −0.08 each).

The methylidyne product (HC≡OsH_2F) in the singlet ground state is clearly more stable than the insertion (CH_3—OsF) and methylidene (CH_2═OsHF) complexes in the quartet and triplet ground states, consistent with the exclusive formation of the product with a carbon—osmium triple bond. The HC≡OsH_2F(S) carbyne is 88 kcal/mol more stable than the reactants (Os(^{5}D) + CH_3F) using B3LYP/6-311++G(3df,3pd)/SDD while CH_3—OsF(Q) and CH_2═OsHF(T) are only 62 and 69 kcal/mol more stable.

Shown in Figure 5 are the Os + CH_3Cl and CH_3Br spectra in the C—H, C—D, and Os—D stretching and low-frequency regions. The product absorptions marked "**y**" in the spectra remain almost the same on vis ($\lambda > 420$ nm) photolysis, but increase ~50% on UV ($240 < \lambda < 380$ nm) photolysis, and sharpen up in the early process of annealing. The C—H stretching absorptions are observed at 3091.0 and 3091.2 cm^{-1} in the CH_3Cl and CH_3Br spectra, only 0.9 and 0.7 cm^{-1} lower than that in the CH_3F spectrum, respectively, and their D counterparts are at 2325.8 and 2325.5 cm^{-1} (H/D ratios of 1.329). The C—H stretching absorptions with considerably higher frequencies than those of normal saturated hydrocarbons suggest that methylidyne products (HC≡OsH_2Cl and HC≡OsH_2Br) are formed in reactions of Os with methyl chloride and bromide. The observed frequencies are compared with the predicted values for the methylidyne complexes (Tables 4 and 5) and display satisfactory agreement as expected.[26]

(27) Doherty, N. M.; Hoffman, N. W. *Chem. Rev.* **1991**, *91*, 553.

Table 4. Observed and Calculated Fundamental Frequencies of HC≡OsH_2Cl Isotopomers[a]

	HC≡OsH_2Cl					DC≡OsD_2Cl				
approx description	obsd	B3LYP, anh[b]	B3LYP	CCSD	int	obsd	B3LYP, anh[b]	B3LYP	CCSD	int
A′ C-H str.	3091.0	3093.0	3243.7	3274.7	27	2325.8	2334.3	2416.1	2439.0	19
A′ OsH_2 str.	2203.6	2207.7	2299.5	2365.8	9	1583.2	1585.5	1632.1	1678.8	14
A′ C≡Os str.		1088.0	1102.5	1106.9	4		1033.3	1049.4	1053.0	5
A′ HCOs bend		917.4	940.5	946.6	14		714.8	732.3	732.8	5
A′ OsH_2 scis.	*c*	743.8	757.9	806.6	15		528.0	538.2	572.6	7
A′ OsH_2 wag	602.8	619.8	625.1	609.9	78	440.9	450.5	452.7	446.1	27
A′ OsCl str.		354.4	356.1	360.8	75		350.5	352.8	356.7	82
A′ COsCl bend		119.4	109.9	116.8	4		107.4	101.8	107.8	3
A″ OsH_2 str.	2164.1	2185.9	2271.7	2336.7	28		1567.7	1610.9	1657.1	5
A″ HCOs bend		887.4	915.6	889.6	1		700.5	718.8	688.9	0
A″ OsH_2 twist	626.4, 624.5	645.5	655.1	604.9	46	448.3	463.5	467.4	438.9	23
A″ OsH_2 rock		198.5	174.4	198.6	1		143.4	132.4	150.3	0

[a] Frequencies and intensities are in cm^{-1} and km/mol. Observed in an argon matrix. Harmonic frequencies are computed with B3LYP/6-311++G(3df, 3pd) or CCSD/6-311++G(2d, p), and the SDD core potential and basis set are used for Os. Intensities are for CCSD. HC≡OsH_2Cl has a C_s structure with two equal Os—H bonds. The symmetry notations are based on the C_s structure. [b] Calculated anharmonic frequencies. [c] Covered by precursor band.

Table 5. Observed and Calculated Fundamental Frequencies of HC≡OsH_2Br Isotopomers[a]

	HC≡OsH_2Br					DC≡OsD_2Br				
approx description	obsd	B3LYP, anh[b]	B3LYP	CCSD	int	obsd	B3LYP, anh[b]	B3LYP	CCSD	int
A′ C—H str.	3091.2	3114.7	3240.3	3274.8	29	2325.5	2346.3	2413.7	2439.4	21
A′ OsH_2 str.	2195.4	2199.9	2293.9	2363.4	35	1579.9	1580.3	1628.1	1677.2	18
A′ C≡Os str.		1085.6	1101.7	1108.9	5		1031.8	1048.5	1054.6	6
A′ HCOs bend	890.1	908.6	936.2	944.3	18		710.4	727.6	730.2	7
A′ OsH_2 scis.		712.1	756.7	809.2	15		516.0	537.1	574.1	7
A′ OsH_2 wag	covered	617.5	624.4	605.4	84	436.3	446.2	450.4	440.0	40
A′ OsBr str.		242.7	243.5	244.0	32		240.7	242.0	242.5	34
A′ COsBr bend		108.5	102.3	105.9	4		98.0	93.8	97.0	3
A″ OsH_2 str.		2176.5	2265.5	2334.2	8		1561.4	1606.5	1655.3	4
A″ HCOs bend		883.9	910.6	891.5	1		696.4	713.1	688.3	0
A″ OsH_2 twist	623.7	640.3	653.9	600.5	43	448.5	459.0	467.2	436.3	21
A″ OsH_2 rock		147.7	168.9	187.7	1		127.1	126.1	140.6	0

[a] Frequencies and intensities are in cm^{-1} and km/mol. Observed in an argon matrix. Harmonic frequencies are computed with B3LYP/6-311++G(3df, 3pd) or CCSD/6-311++G(2d, p), and the SDD core potential and basis set are used for Os. Intensities are for CCSD. HC≡OsH_2Br has a C_s structure with two equal Os—H bonds. The symmetry notations are based on the C_s structure. [b] Calculated anharmonic frequencies.

Table 6. Observed and Calculated Frequencies of Strong Absorptions of CH_3C≡OsH_3 Isotopomers in the Ground ^{2}A′ Electronic State[a]

	CH_3C≡OsH_3					CD_3C≡OsD_3				
approx description	obsd	B3LYP, anh[b]	B3LYP	CCSD	int	obsd	B3LYP, anh[b]	B3LYP	CCSD	int
A′ OsH_2 str.	**1982.3**, 1978.9	2092.4	2214.5	2285.4	57	**1419.7**, 1417.6	1509.5	1572.2	1622.1	30
A′ OsH str.	**1813.3**, 1810.6	1767.1	1812.2	1868.8	293	**1313.9**, 1305.7	1264.9	1286.4	1326.2	142
A′ C≡Os str.		1435.4	1468.8	1492.9	8		1433.8	1465.0	1500.8	6
A′ CH_3 rock		984.0	1025.3	1062.8	9		800.7	816.9	849.5	6
A′ OsH_3 deform	755.6	855.0	793.5	882.3	31	551.1	618.0	590.5	627.2	20
A″ OsH_2 str.		2061.2	2177.9	2251.8	15		1477.0	1544.7	1597.1	8
A″ CH_3 scis.		1408.7	1458.8	1499.9	11		1023.8	1049.8	1079.3	5

[a] Frequencies and intensities are in cm^{-1} and km/mol. Observed in an argon matrix. Harmonic frequencies are computed with B3LYP/6-311++G(3df, 3pd) or CCSD/6-311++G(2d, p), and the SDD core potential and basis set are used for Os. Intensities are for CCSD. CH_3C≡OsH_3 has a C_s structure with two equal Os—H bonds. The symmetry notations are based on the C_s structure. [b] Calculated anharmonic frequencies.

A weak Os—H stretching absorption and its D counterpart are observed at 2203.6 (not shown) and 1583.2 cm^{-1} (H/D ratio of 1.392) in the CH_3Cl and CD_3Cl spectra, and the former is assigned to the A′ OsH_2 stretching mode of HC≡OsH_2Cl. Another weak Os—H stretching absorption at 2164.1 cm^{-1} is designated for the A″ OsH_2 stretching mode without observation of the D counterpart. In the low-frequency region, a product absorption at 624.5 cm^{-1} reveals a D shift of −176.2 cm^{-1} (H/D ratio of 1.393), and it is assigned to the OsH_2 twisting mode. A stronger product absorption at 602.8 cm^{-1} has the D counterpart at 440.9 cm^{-1} (H/D ratio of 1.367) and is attributed to the OsH_2 wagging mode. The observed frequencies exhibit satisfactory agreement with the predicted values (Table 4) and substantiate the formation of HC≡OsH_2Cl.

Likewise a weak product absorption and its D counterpart at 2195.4 and 1579.9 cm^{-1} (H/D ratio of 1.390) in the methyl bromide spectra are assigned to the A′ OsH_2 and OsD_2 stretching modes. In the low-frequency region, a product absorption at 890.1 cm^{-1} is assigned to the H—C—Os bending mode without observation of the D counterpart. In the further low-frequency region, the absorption at 623.7 cm^{-1} shows a D shift of −175.2 cm^{-1} (1.391) and is assigned to the OsH_2 twisting mode on the basis of the large D shift. The observed band at 436.3 cm^{-1} in the CD_3Br spectrum is attributed to the OsH_2 wagging mode while the H counterpart is believed to be overlapped by a precursor band. The observed frequencies correlate well with the predicted values for HC≡OsH_2Br (Table 5).

The CCSD structures of the methylidyne complexes with C_s symmetry are shown in Figure 7. The long Os—H bond of HC≡OsH_3 is replaced with the Os—F bond, and the Os—H bond lengths (both 1.576 Å) are slightly longer than that (1.563 Å) of the trihydrido Os complex prepared from CH_4. The low

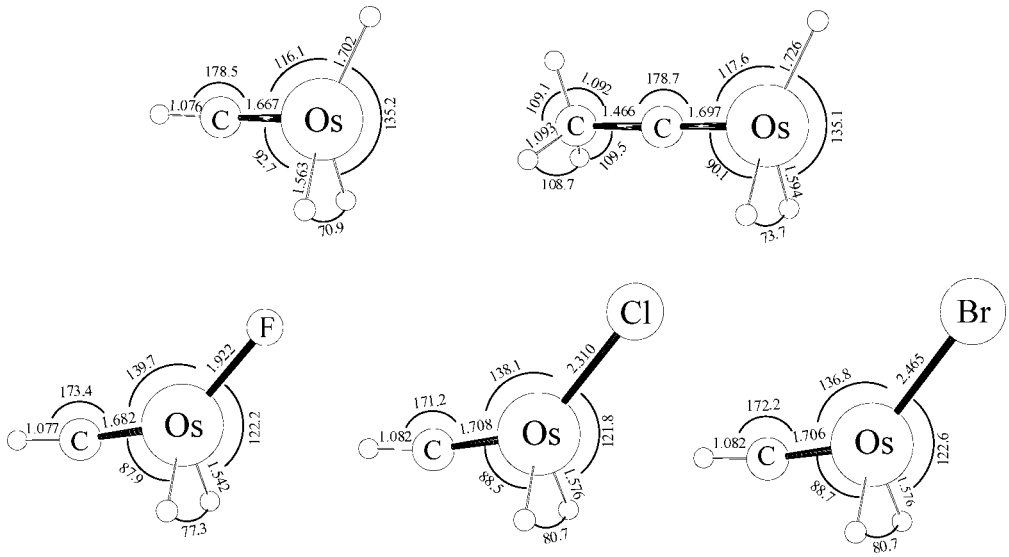

Figure 7. The CCSD structures of $HC{\equiv}OsH_3$, $HC{\equiv}OsH_2F$, $HC{\equiv}OsH_2Cl$, $HC{\equiv}OsH_2Br$, and $CH_3{-}C{\equiv}OsH_3$. While 6-311++G(3df,3pd)/SDD is used for $HC{\equiv}OsH_3$ and $HC{\equiv}OsH_2F$, a smaller basis set (6-311++G(2d,p)) is used for the others. The bond lengths and angles are in Å and deg. They all have C_s structures in their $^1A'$ ground states, and particularly $HC{\equiv}OsH_3$ and $CH_3{-}C{\equiv}OsH_3$ have one long and two shorter equal Os—H bonds. As a result, the H—C—Os and C—C—Os moieties are slightly bent.

absorption intensities of the Os—H stretching bands are again rationalized by the relatively low negative charges on the hydrogen atoms bonded to the metal center, Mulliken charges of −0.07 for both $HC{\equiv}OsH_2Cl$ and $HC{\equiv}OsH_2Br$. The methylidyne complexes are clearly the most stable among the plausible products. $HC{\equiv}OsH_2Cl$(S) is 91 kcal/mol lower than the reactants at the level of B3LYP/6-311++G(3df,3pd)/SDD while $CH_3{-}OsCl$(Q) and $CH_2{=}OsHCl$(T) are 67 and 73 kcal/mol lower, respectively. $HC{\equiv}OsH_2Br$(S) is 93 kcal/mol more stable than the reactants while $CH_3{-}OsBr$(Q) and $CH_2{=}OsHBr$(T) are 69 and 75 kcal/mol more stable, respectively.

Os + C_2H_6. Figure 6 illustrates product spectra from the Os and ethane reaction in the Os—H and Os—D stretching and low-frequency regions. The product absorptions marked "**y**" remain unchanged on vis ($\lambda > 420$ nm) irradiation, but increase ~25% on UV ($240 < \lambda < 380$ nm) irradiation. They also increase slightly more on full arc ($\lambda > 220$ nm) irradiation and sharpen in the early stage of annealing. Parallel to those in the CH_4 spectra, unique strong absorptions split by the matrix are observed at 1813.3 and 1810.6 cm^{-1}, which are 35.4 and 38.1 cm^{-1} lower than the frequency of the main Os—H stretching absorption in the CH_4 spectrum (Figure 2 and Supporting Information Figure S1), respectively. The magnitude of the red shift upon methyl substitution is compared with that of 23.6 cm^{-1} in the previous Re study.[9] The D counterparts are observed at 1305.7 and 1303.9 cm^{-1} (H/D ratios of 1.389), which are 24.5 and 26.3 cm^{-1} lower than the corresponding Os—D stretching frequency in the CD_4 spectrum. The strong Os—H stretching absorption with exceptionally low frequency suggests an unusually long Os—H bond similar to the product in the Os + CH_4 and corresponding Re systems.[9]

The methylidyne complex ($CH_3C{\equiv}OsH_3$) is again the most stable among the plausible products of the Os + C_2H_6 reaction, which is 47 kcal/mol more stable than the reactants at the B3LYP level of theory. The structure of the trihydrido product shown in Figure 7 has C_s symmetry with a long (1.726 Å) and two equal short (1.594 Å) Os—H bonds, whereas the monohydrido insertion product ($CH_3CH_2{-}OsH$) in its triplet ground state is 31 kcal/mol lower than the reactants and would show a Os—H stretching absorption at around 2100 cm^{-1} after considering the scale factor (0.96), which is almost 300 cm^{-1} higher than the frequency of the strong Os—H stretching absorption. $CH_3{-}CH{=}OsH_2$(S), another plausible product, is 43 kcal/mol lower than the reactants, and the two Os—H stretching bands would appear at around 2110 cm^{-1} with similar intensities and about 40 cm^{-1} apart. A possible cyclic product, $(CH_2)_2OsH_2$(T), is 31 kcal/mol more stable than the reactants and would show two Os—H stretching absorptions at around 2010 cm^{-1} with similar intensities and about 50 cm^{-1} apart. Other plausible products, such as $(CH_3)_2Os$, CH_2CHOsH_3, $CHCHOsH_4$, and $HC{\equiv}COsH_5$, were also examined, but none of them is predicted as stable as $CH_3C{\equiv}OsH_3$ or reproduces the observed strong Os—H stretching band in the exceptionally low frequency region. No significant additional Os—H absorptions are observed in this diagnostic region of the spectrum (Figure S1, Supporting Information).

The observed strong Os—H stretching absorptions at 1813.3 and 1810.6 cm^{-1} are assigned to the stretching of the long Os—H bond (1.726 Å) of the methylidyne product. Another Os—H stretching absorption, which is much weaker than the strong one at 1813.3 cm^{-1}, is observed at 1982.3 cm^{-1} and its D counterpart is at 1419.7 cm^{-1} (H/D ratio of 1.396). On the basis of the higher frequency, they are assigned to the A′ stretching mode of the shorter Os—H bonds (1.594 Å). The lower and higher absorption intensities of the high and low stretching frequency modes again originate from the smaller and larger negative charges on the hydrogen atoms. Mulliken charges of −0.11 and −0.35 with use of B3LYP/6-311++G(3df,3pd)/SDD provide a reliable prediction of the relative charges on these atoms (Table 7). The CCSD calculation overestimates the higher Os—H stretching mode by 15% and the lower unique Os—H stretching mode by only 3%, and we do not understand the reason for this difference.

Finally, another product absorption and its D counterpart at 755.6 and 551.1 cm^{-1} (H/D ratio of 1.371) in the low-frequency region are assigned to the OsH_3 deformation mode. The broadband at 530 cm^{-1} due to ethyl radical is a common photolysis product in ethane experiments with many laser-ablated metals.[9,28]

(28) Cho, H.-G.; Andrews, L. *J. Phys. Chem. A* **2008**, *112*, 1519. (group 4 + C_2H_6).

Table 7. Methylidyne C—H Stretching Frequencies and Bond Properties[a]

properties	HC≡CH	HC≡OsH_3	HC≡OsH_2F	HC≡OsH_2Cl	HC≡OsH_2Br	CH_3CH_3
obsd	3284[b]	3117.8	3091.9	3091.0	3091.2	2979.3
calcd(harm)	3412.3	3131.2	3101.8	3093.0	3114.7	3027.3
calcd(anharm)		3243.8	3246.8	3243.7	3240.3	
obsd/calcd(harm)	0.962	0.961	0.952	0.953	0.953	0.984
s-character (C—H)[c]	47.82	46.81	45.17	45.48	45.54	23.46
s-character (C—M)[c]	52.34	53.08	54.70	54.38	54.31	29.75
q(H)[d]	0.222	0.181	0.177	0.180	0.181	0.190
q(H)[d]		−0.107, 0.091	0.050	0.050	0.047	
q(H)[d] or *q*(X)[d]		−0.285	−0.619	−0.444	−0.402	
q(C)[d]	−0.222	−0.158	−0.135	−0.081	−0.077	−0.570
q(Os)[d]		0.278	0.478	0.245	0.204	
r(C—H)[e]	1.062	1.081	1.081	1.081	1.082	1.091
r(C—C) or (C—M)[e]	1.196	1.698	1.707	1.702	1.700	1.527
∠HCOs[f]	180.0	162.4	170.8	171.6	171.9	111.3

[a] Frequencies are in cm^{-1}. Harmonic frequencies are computed with 6-311++G(3df, 3pd), and the SDD core potential and basis set are used for Os. [b] Reference 30. [c] s-character of the carbon atom in the bond. [d] Natural charge. *q*(H), first is H to C, second is Os—H pair, and third is unique long Os—H. [e] Bond length in Å. [f] Angle in deg.

Methylidyne C—H Stretching Absorption. The diagnostic methylidyne C—H stretching absorptions of the Os complexes are observed as shown in Figures 1, 4, and 5. The weak but important methylidyne C—H stretching bands are often covered by other much stronger absorptions in this region.[23] These simple methylidyne products with no interfering ligand chromophores and limited precursor absorptions in this region allow for observation of the elusive C—H stretching band of the H—C≡M moiety. The frequencies are about 200 cm^{-1} higher than those of saturated hydrocarbons and signify interaction with a carbon−osmium triple bond, which increases the s character of the C—H bond,[23] but the frequencies are still much lower than that of acetylene. Unlike in acetylene, the difference in electronegativity between the carbon and osmium atoms (2.5 and 2.2 in the Pauling scale) polarizes the C≡Os bond and allocates more s character in the carbon−metal bond, leaving less s character in the C—H bond. The close relationship between the methylidyne C—H stretching frequency and the amount of s character is examined in the previous Re studies.[29]

The observed methylidyne C—H stretching frequencies are compared with the amount of natural bond orbital (NBO)computed s characters in Table 7. The much higher C—H stretching frequency of acetylene (3284 cm^{-1} and the IR-inactive symmetric stretching mode some 90 cm^{-1} higher)[30] is consistent with highest s character (47.82%), and the higher frequency of HC≡OsH_3 (3117.8 cm^{-1}) relative to that of HC≡OsH_2X is also accounted for with its higher s character (46.81%). The C—H stretching frequencies of HC≡OsH_2X (3091.9, 3091.0, and 3091.2 cm^{-1} for F, Cl, and Br) are similar to each other, and so are the s characters (45.17%, 45.48%, and 45.54%). Evidently the high electronegativity of F leads to the lowest s character among the halogenated products, and therefore, the tendency of increasing frequency with the s character does not exactly hold among the halogenated products. The much lower C—H stretching frequency of ethane is also accompanied by the much lower s character (23.46%).

Although not as consistent as in the Re case, the relatively high frequency and its variation of the methylidyne C—H stretching absorption are still roughly in line with the amount of s character. Complications from more than one halogen ligand also tend to break down the relationship between the methylidyne C—H stretching frequency and the s character,[11] suggesting that a high ligand electronegativity affects the electronic configuration of the C—H bond in such a way to deviate from the relationship between the C—H stretching frequency and the s character.

Structure. The methylidyne complexes investigated here all have C_s structures in their singlet ground states (Figure 7). Although HC≡OsH_3 has a computed C_1 structure with the B3LYP or BPW91 density functionals, it has C_s structures with the higher level MP2 and CCSD ab initio methods and the same large basis. All other complexes examined in this study also have C_s structures at all levels of theory employed. The C_s structures of HC≡OsH_3 and CH_3—C≡OsH_3 are similar to the C_s structures of the corresponding Re methylidyne complexes,[9] but contrast the C_{3v} structures of the Group 6 metal methylidyne complexes (HC≡MoH_3 and HC≡WH_3) in their singlet ground states.[12,31] One of the Os—H bonds in the structures of HC≡OsH_3 and CH_3C≡OsH_3 is tilted more with a longer bond length than the other two. In the halogenated complexes, the longer Os—H bond is replaced by the Os—X bond.

It is interesting to compare the structures of the three complexes HC≡WH_3, HC≡ReH_3, and HC≡OsH_3, which differ by two 5d valence electrons. Notice that the distortion from C_{3v} is more in the latter Os complex with two extra electrons than for the Re complex with a single lone electron (compare Figure 4 in ref 9a). Notice also that the long–short metal hydride bond difference is greater for the Os complex (0.166 Å) as compared to Re (0.071 Å). This is because two extra electrons in the HOMO are antibonding for the long Os—H bond (see the HOMO in Figure 8), but only one is antibonding for Re and none for the W complex.

The methylidyne H—C bond lengths of 1.076–1.082 Å are similar to those of 1.079–1.083 Å for the previously studied Re complexes and those of 1.076 and 1.081 Å determined for H—C≡W[4] and HC≡WH_3,[31] respectively. The observed C—H frequency of HC≡OsH_3 is 16 cm^{-1} higher than that of HC≡ReH_3, whose frequency is in turn 18 cm^{-1} above that of HC≡WCl_3 and 29 cm^{-1} higher than that of HC≡WH_3.[31,32] The short Os—H bond length varies in the range of 1.542 to 1.594 Å as shown in Figure 8, which can be compared with 1.571 and 1.565 Å measured for $[OsH(=C=C=CPh_2)(CH_3CN)_2(P^iPr_3)_2]BF_4$ and H(μ-H)$Os_3(CO)_{10}$(HN=CPh_2), respec-

(29) Reed, A. E.; Curtiss, L. A.; Weinhold, F. *Chem. Rev.* **1988**, *88*, 899.

(30) Herzberg, G. *Infrared and Raman Spectra*; D. Van Nostrand: Princeton, NJ, 1945.

(31) Cho, H.-G.; Andrews, L.; Marsden, C *Inorg. Chem.* **2005**, *44*, 7634. and references therein (W + CH_4).

(32) Lyon, J. T.; Cho, H.-G.; Andrews, L. *Organometallics* **2007**, *26*, 6373. (W + $CHCl_3$).

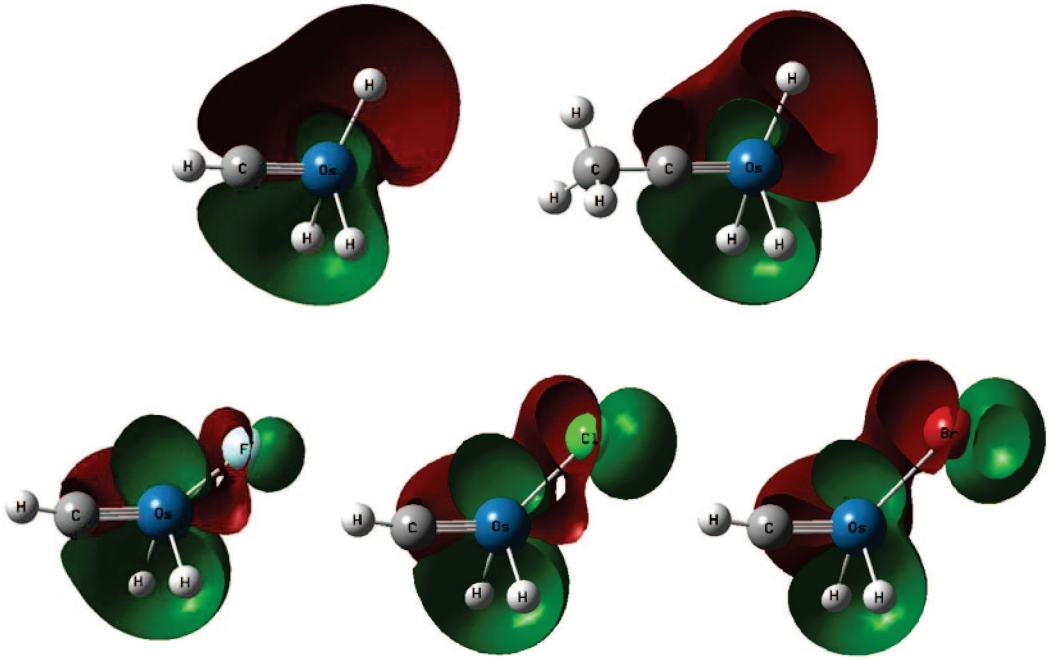

Figure 8. The HOMOs of $HC{\equiv}OsH_3$, $CH_3{-}C{\equiv}OsH_3$, $HC{\equiv}OsH_2F$, $HC{\equiv}OsH_2Cl$, and $HC{\equiv}OsH_2Br$. Plots from CCSD calculation for $HC{\equiv}OsH_3$ and B3LYP for all others. Notice that the lone electron pair on the Os atom provides antibonding character to one of the Os—H bonds of the trihydrido complexes ($HC{\equiv}OsH_3$ and $CH_3{-}C{\equiv}OsH_3$) or the Os—X bond of the halogenated derivatives. The antibonding character elongates the Os—H (or Os—X) bond and increases the C—Os—H angle.

tively.[25] The C≡Os bond length increases on substitution of halogen (from 1.667 to 1.682, 1.708, and 1.706 Å for F, Cl, and Br, respectively), and substitution of a methyl group on the carbon atom also increases the C≡Os bond length (from 1.667 to 1.697 Å). Our calculated C≡Os bond lengths of 1.667–1.708 Å may be compared with the C≡Os bond lengths of 1.694 and 1.708 Å determined for the osmium carbyne complexes reported in ref 7b and of 1.733(9), 1.733(6), and 1.73(1) Å measured for $[OsH(\eta^5\text{-}C_5H_5)(\equiv C{-}Ph)(P^iPr_3)]PF_6$, $[OsH(\equiv CCH{=}CPh_2)(H_2O)_2(P^iPr_3)_2][BF_4]_2$, and $[Os(NH_3)_5(\equiv CPh)](OTf)_3$, respectively.[33]

The low symmetry of the Re complexes is accounted for by the Jahn–Teller effect, which eliminates the double degeneracy of the electronic states, giving the methylidyne complexes nondegenerate $^2A'$ ground states, and as a result, lowers the molecular symmetry from C_{3v} to C_s.[9,11] Unlike the Re case, the Os methylidynes investigated in the present study all have singlet ground states with a lone electron pair. Evidently the lone electron pair gives a significant amount of antibonding character to one of the Os—H bonds, leading to significant elongation of the bond. Figure 8 shows the HOMO of $HC{\equiv}OsH_3$(S), where a nodal plane bisects the long Os—H bond. The weak Os—H bond with a high negative charge on the hydrogen atom results in the strong Os—H stretching absorption at the exceptionally low frequency.

Mechanism. Osmium atoms excited in the laser ablation process react with the methane, methyl halide, and ethane precursors during the codeposition process on the surface of the condensing matrix, and similar reactions occur during irradiation of the solid matrix. As described above, only the methylidyne complexes are trapped while C—H or C—X insertion is believed to occur first in the reactions. It is notable that even reaction products ~20 kcal/mol higher than the most stable have often been formed during reactions of excited transition-metal reactions with CH_4 and methyl halides or photolysis afterward and trapped in the solid argon matrix.[12] While the methylidyne complexes are computed to be the most stable species among the plausible products in the Os systems investigated in this study, the high preference for the carbon–osmium triple bond is clear and analogous to that found for rhenium.[9]

$$Os^* + CH_3X \rightarrow [CH_3{-}OsX]^* \rightarrow [CH_2{=}OsHX]^* \rightarrow HC{\equiv}OsH_2X \quad (1)$$

The Os atom, electronically excited in the laser ablation process or by ultraviolet irradiation, undergoes C—H or C—X insertion, and α-hydrogen migration follows, as given in reaction 1. This suggests that the H migration process occurs swiftly requiring a very small amount of activation energy, faster than relaxation of the energized intermediates in the matrix cage. As a matter of fact, geometry optimization for the possible insertion and methylidene products often ends up with the structure of the methylidyne complex (e.g., Os + CH_3F and Os + CH_3Cl systems). The present results also indicate that the intersystem crossings occur readily from the starting quintet state ($Os(^5D_4)$ + CH_4) to the more stable singlet state in these Os systems.

Finally, we note that $HC{\equiv}OsH_3$ is sensitive to visible light decreasing about half under >420 nm irradiation but increasing on 240–380 nm irradiation. This could be due to a photoreversible α-hydrogen transfer process like that documented for the $HC{\equiv}MoH_3$ and $HC{\equiv}WH_3$ methylidynes[12,31] or to a simple photodissociation of $HC{\equiv}OsH_3$ followed by its reformation via equation 1 (X = H).

(33) (a) Esteruelas, M. A.; González, A. I.; López, A. M.; Onate, E. *Organometallics* **2003**, *22*, 414. (b) Bolano, T.; Castarlenas, R.; Esteruelas, M. A.; Modrego, F. J.; Onate, E. *J. Am. Chem. Soc.* **2005**, *127*, 11184. (c) Hodges, L. M.; Sabat, M. S.; Harman, W. D *Inorg. Chem.* **1993**, *32*, 371. (C≡Os bond length).

Conclusions

Parallel to the Re case,[9] osmium hydride methylidyne complexes, $HC{\equiv}OsH_3$, $HC{\equiv}OsH_2F$, $HC{\equiv}OsH_2Cl$, $HC{\equiv}OsH_2Br$, and $CH_3C{\equiv}OsH_3$, are produced in reactions of laser-ablated Os atoms with the corresponding small alkanes and methyl halides. These methylidyne complexes have lower computed energies relative to other plausible C—H activation products. The observed vibrational characteristics correlate with the predicted values for the methylidyne complexes.

As in the previous Re studies, the diagnostic methylidyne C—H stretching absorptions are about 200 cm^{-1} higher than those of normal saturated hydrocarbons. These are clearly observed with isotopic effects in the methane and methyl halide spectra, although such bands in typical organometallic compounds are difficult to observe due to low intensity and other interfering absorptions. While the observed frequencies are basically consistent with the amount of NBO s character in the C—H bond, the trend deviates with fluorine. Polarization in the C≡Os bond is believed to shift the s character from the C—H to the triple bond, leading to the C—H stretching frequency lower than that of acetylene.

The methylidynes have a C_s structure. The CH_4 and C_2H_6 products have one long and two equal shorter Os—H bonds, and the longer Os—H bond is replaced by an Os—X bond in the halogenated product. The lone electron pair on the Os atom evidently provides antibonding character for one of the Os—H bonds to elongate, and the most intense Os—H stretching absorption at an exceptionally low frequency observed in the spectrum originates from the stretching mode of the longer Os—H bond and the high negative charge on the hydrogen atom.

Acknowledgment. We gratefully acknowledge financial support from NSF Grant CHE 03-52487 to L.A., and the use of the computing system of the KISTI Supercomputing Center is also greatly appreciated.

Supporting Information Available: Two tables of calculated frequencies and two additional figures of matrix infrared spectra. This material is available free of charge via the Internet at http://pubs.acs.org.

OM701041U